PennState
College of Earth
and Mineral Sciences

Influence of Intentional Pores on Tensile Behavior of Stainless Steel 316L Manufactured with Laser-Powder Bed Fusion

Theresa C. Novak[1] , Alexander E. Wilson-Heid[1] , & Allison M. Beese[1,2]
1 Department of Materials Science and Engineering, Pennsylvania State University, University Park, PA 16802, USA
2 Department of Mechanical Engineering, Pennsylvania State University, University Park, PA 16802, USA

Department of Materials
Science and Engineering

Project Background and Motivation

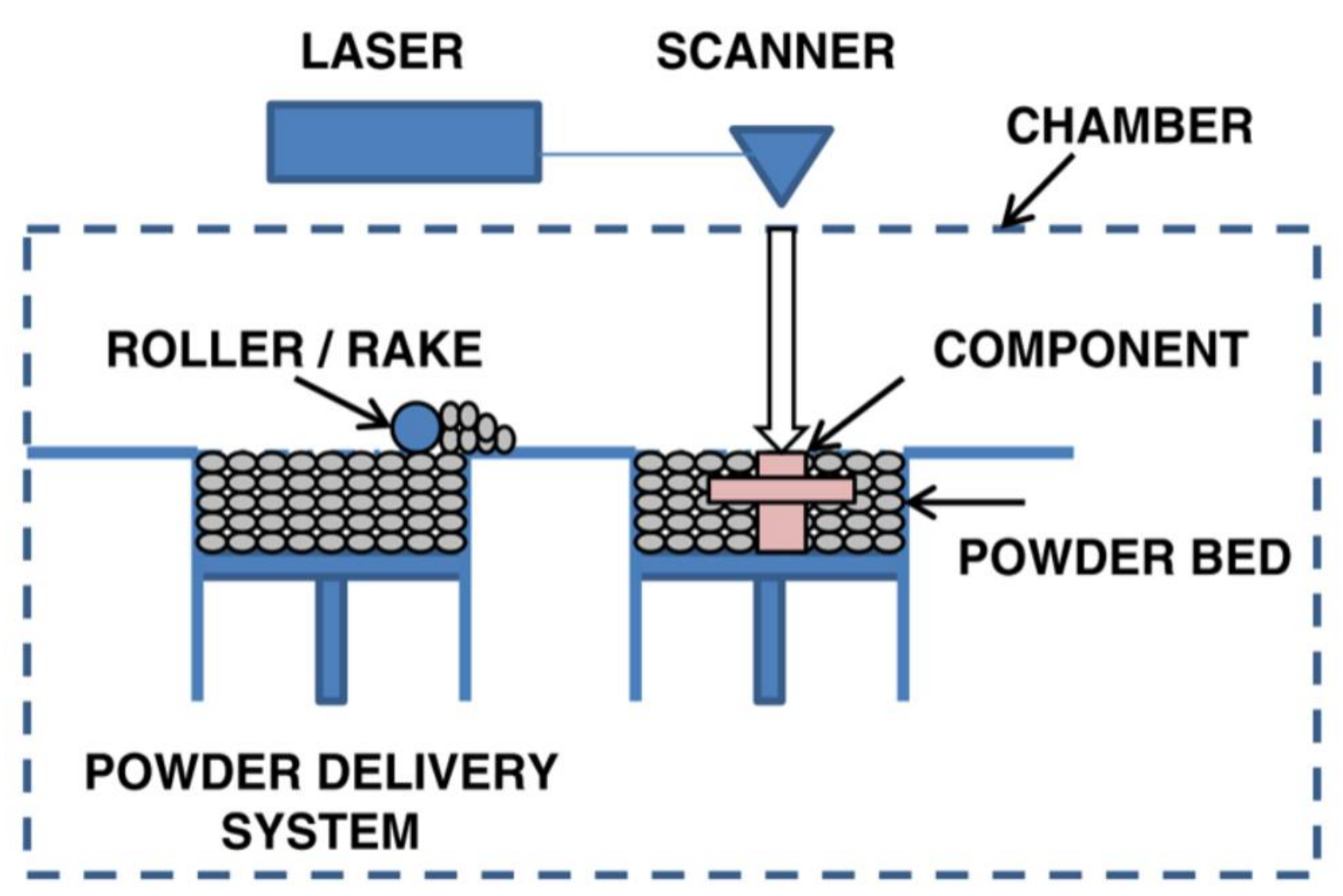

Fig. 1: Schematic of the laser-powder bed fusion additive manufacturing process used to fabricate the SS316L samples in this experiment [1]

As illustrated in **Fig. 1**, the laser-powder bed fusion (L-PBF) additive manufacturing (AM) method employs a laser heat source to melt the intentionally designed areas after a roller deposits a thin layer of powder across the original build plate. This 2D process is repeated to fuse the layers until the 3D piece has been fully constructed. Throughout this procedure, samples may develop internal porosity as a result of processing or raw material defects. These defects include gas entrapment, keyholing, or lack-of-fusion (LoF). LoF defect pores occur when the subsequent layer(s) do not fuse together properly, substituting an empty void in place of the designed solidified material. These pores can range from 15 to 600 µm in length and form in irregular morphologies, usually with sharp edges that induce stress concentration. Cracking stems from these LoF pores and the stress concentration sites are detrimental to the tensile ductility of a specimen. Quantifying this negative impact highlights the defect tolerance of AM while characterizing the effect of porosity on the mechanical behavior.

Experimental Fabrication and Process

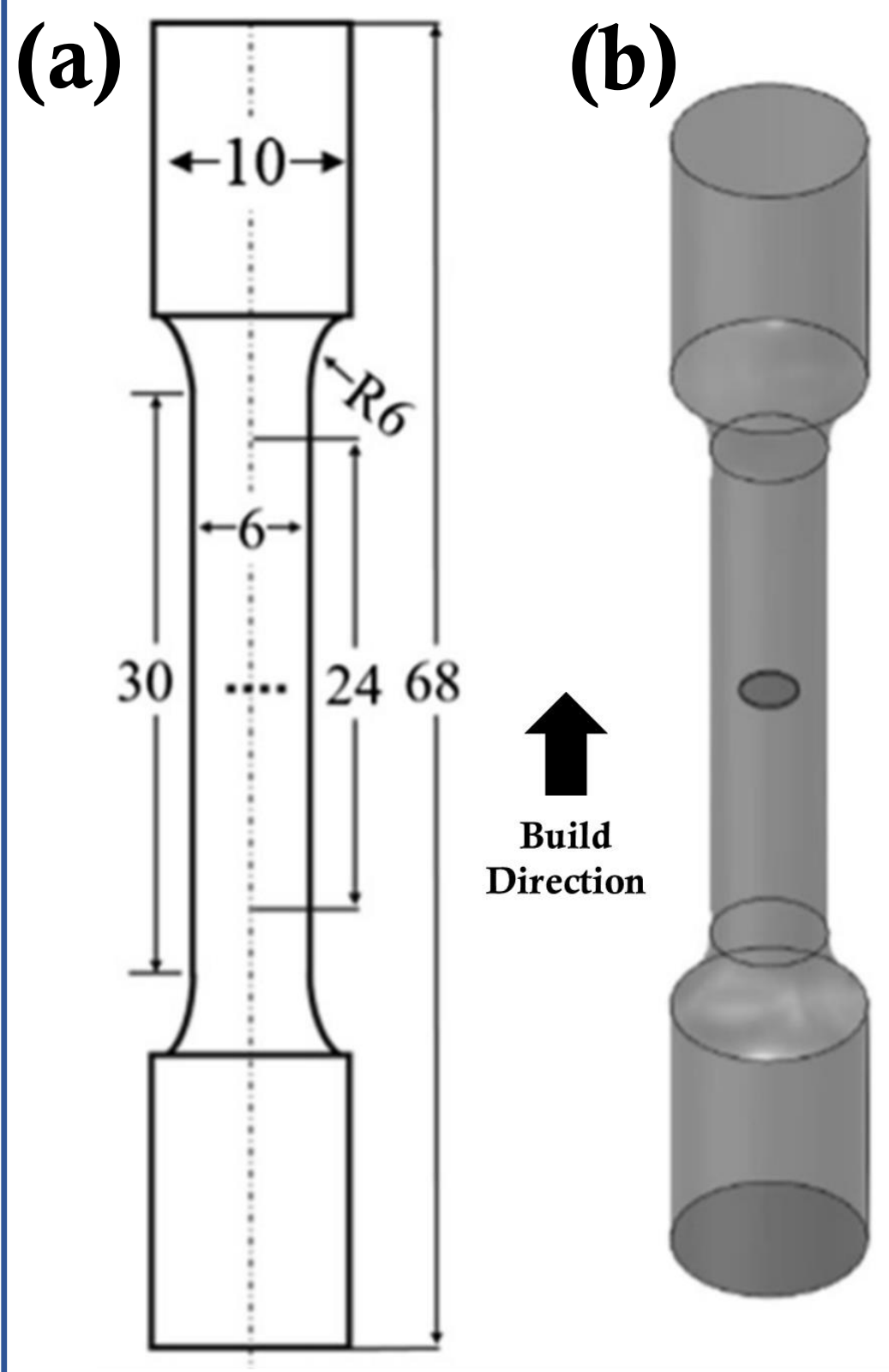

Material: Stainless Steel 316L
Manufacturing Process: Laser-Powder Bed Fusion
Intentionally Designed Internal Porosity: "Penny-shaped" cylindrical pores modeled after LoF pores constructed in the center of the samples. 180 µm tall with eleven different diameters ranging 150 to 4800 µm inside 6 mm gauge diameter (**Fig. 2**).
Porosity Evaluation Techniques:

- Destructive Optical Microscopy
- Nondestructive Archimedes Density Method
- Nondestructive 2D Radiography
- Nondestructive X-ray Computed Tomography(CT)
- Uniaxial Tension Testing

Fig. 2: (Dimensions in mm) **(a)** Uniaxial tension specimen with intentionally introduced pore (indicated by dashed horizontal line), **(b)** 3D CAD rendering of a tensile sample with an internal penny-shaped pore [2]

Destructive 2D-Optical Microscopy

Fig. 3: (a) 2D optical microscopy image of a polished cross-section of a witness sample (Fig (1800 µm pore diameter) **(b)** Comparison of the 2D optical microscopy and radiography as related to their similarity with the pore diameter measured in the 3D X-ray CT analysis using percent difference [2]

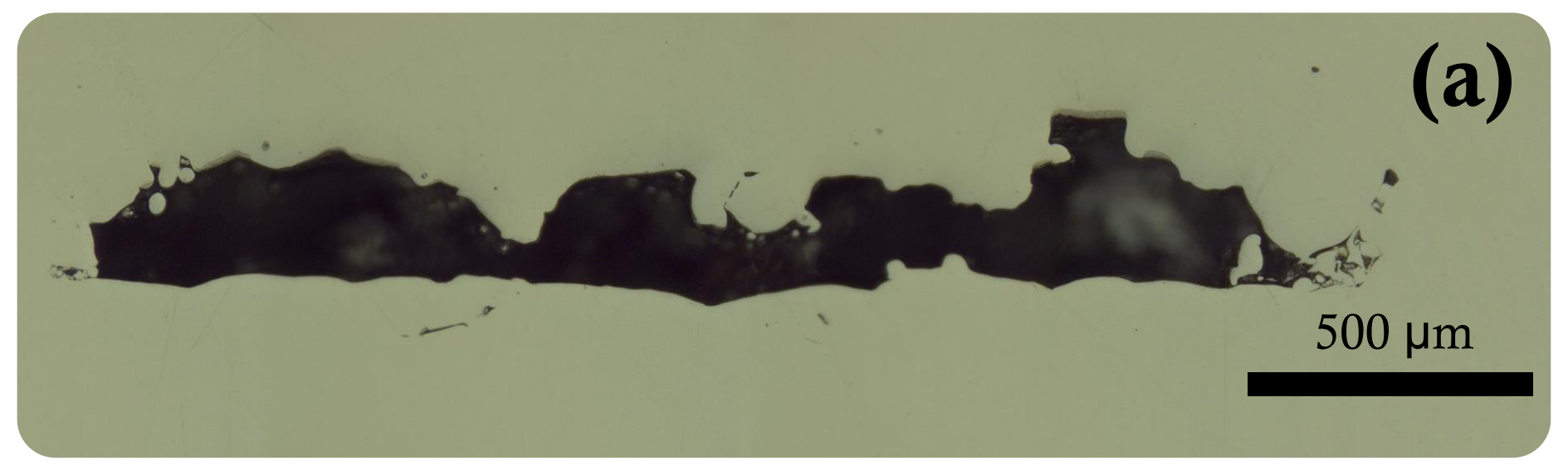

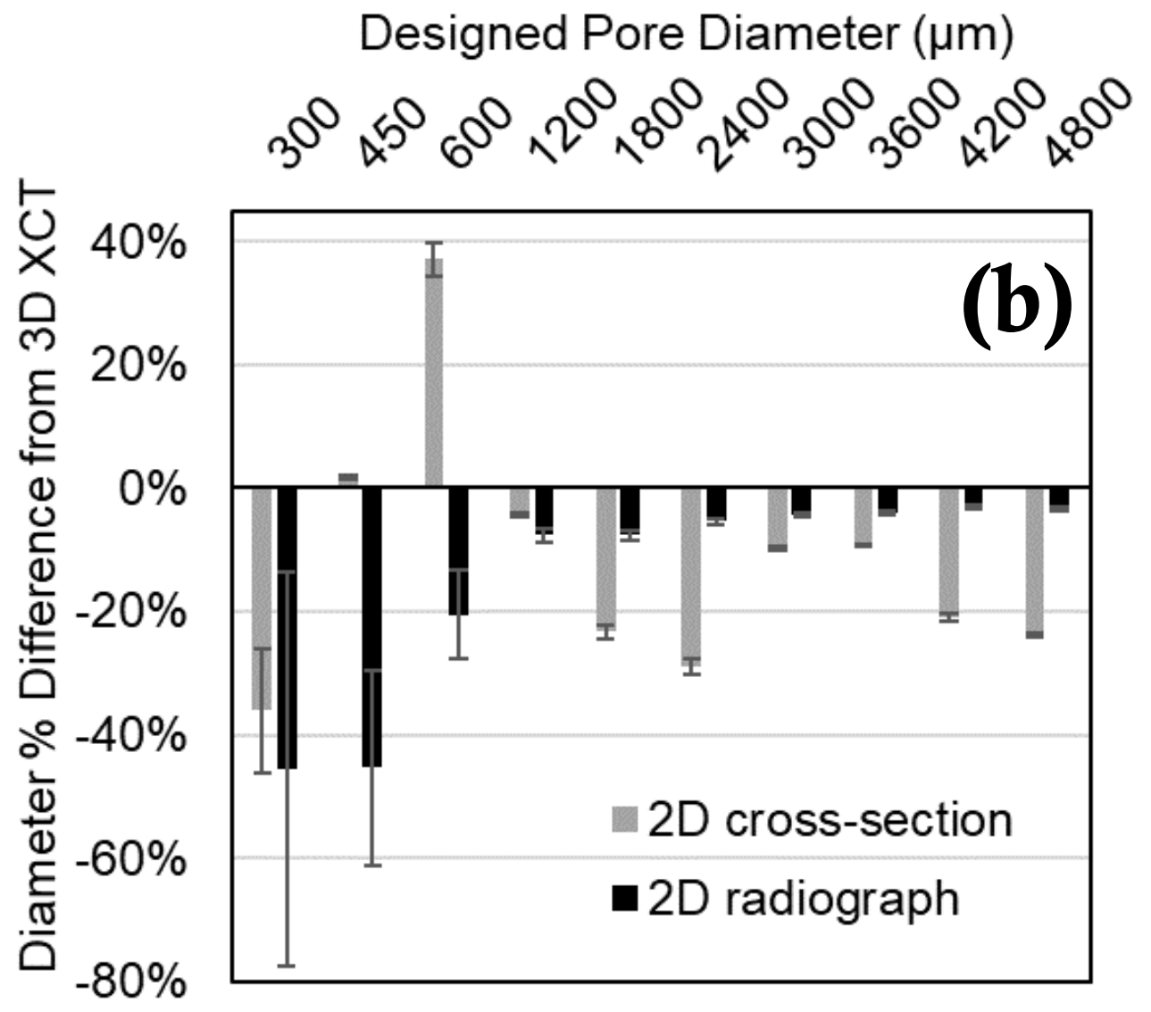

Archimedes Density

Archimedes Method, a nondestructive technique, reveals the density and porosity of the tensile specimens using the following equation with all measurements (**Table 1**) taken five times:

$$\rho = \frac{m_{dry} \times \rho_{theor}}{m_{soak} - m_{sub}}$$

Variable	Identification
m_{dry}	mass of dry samples
m_{soak}	mass of samples patted dry after submersion in water and placed in vacuum for 24 hrs (to allow water to permeate the pores)
m_{sub}	mass of samples submerged in water
ρ_{theor}	7.99 g/cm^3 (assumed for density of SS316L)

Table 1: Archimedes Density variable and its identification

2D Radiography and X-ray CT

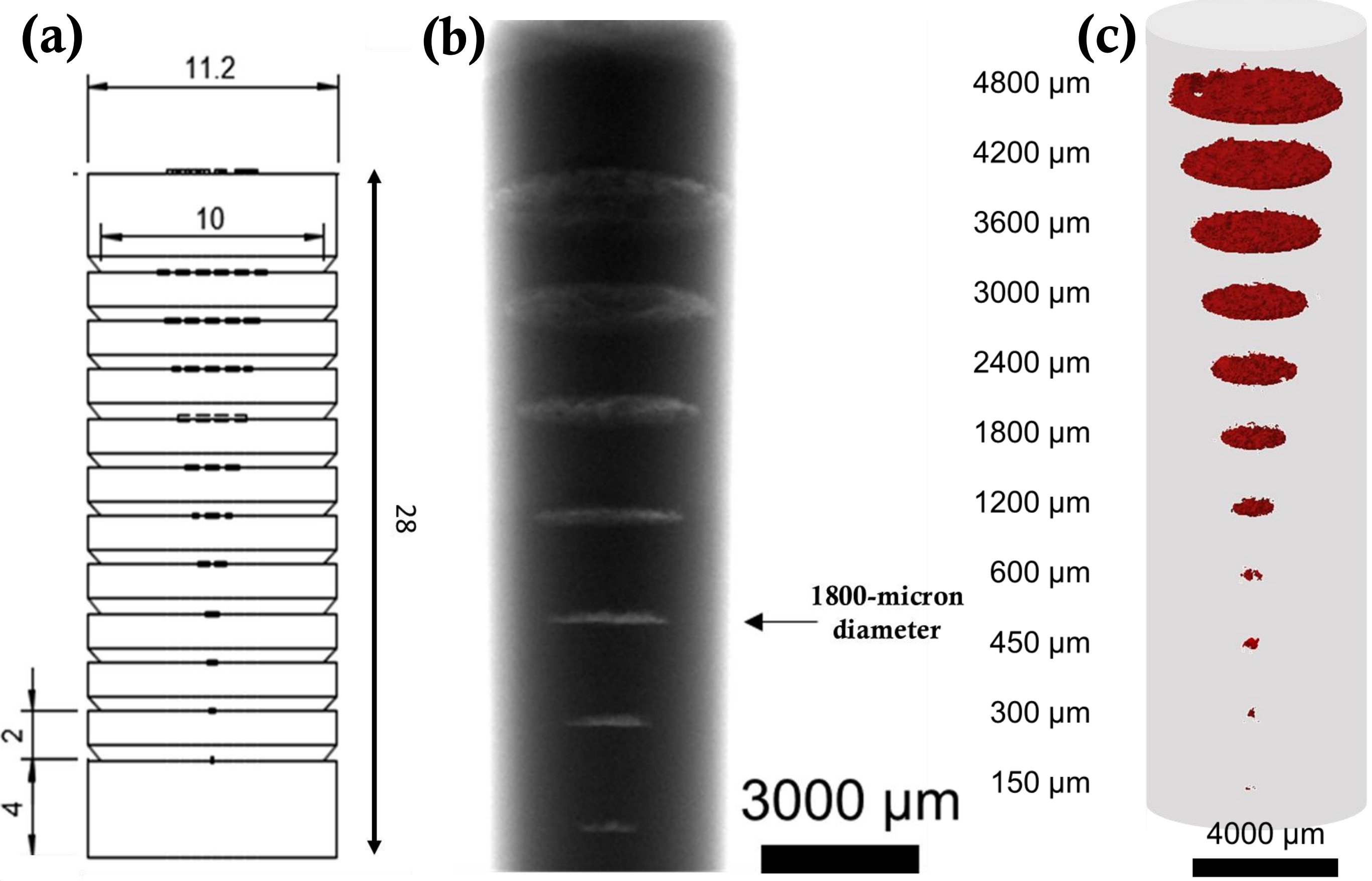

Fig. 4: (a) Dimensions in mm. CAD drawing of witness sample containing pores of diameter 150 µm closest to the baseplate and the 4800 µm farthest from the baseplate.
(b) 2D radiograph image centered at the 1800 µm diameter pore. Each pore was centered with respect to the X-ray source for dimensional analysis to eliminate skewing, as seen in the larger pores in this image
(c) 3D X-ray CT reconstruction of the eleven pores in the witness sample within the 6 mm diameter cylinder **[2]**

Uniaxial Tension Testing – Stress vs. Strain

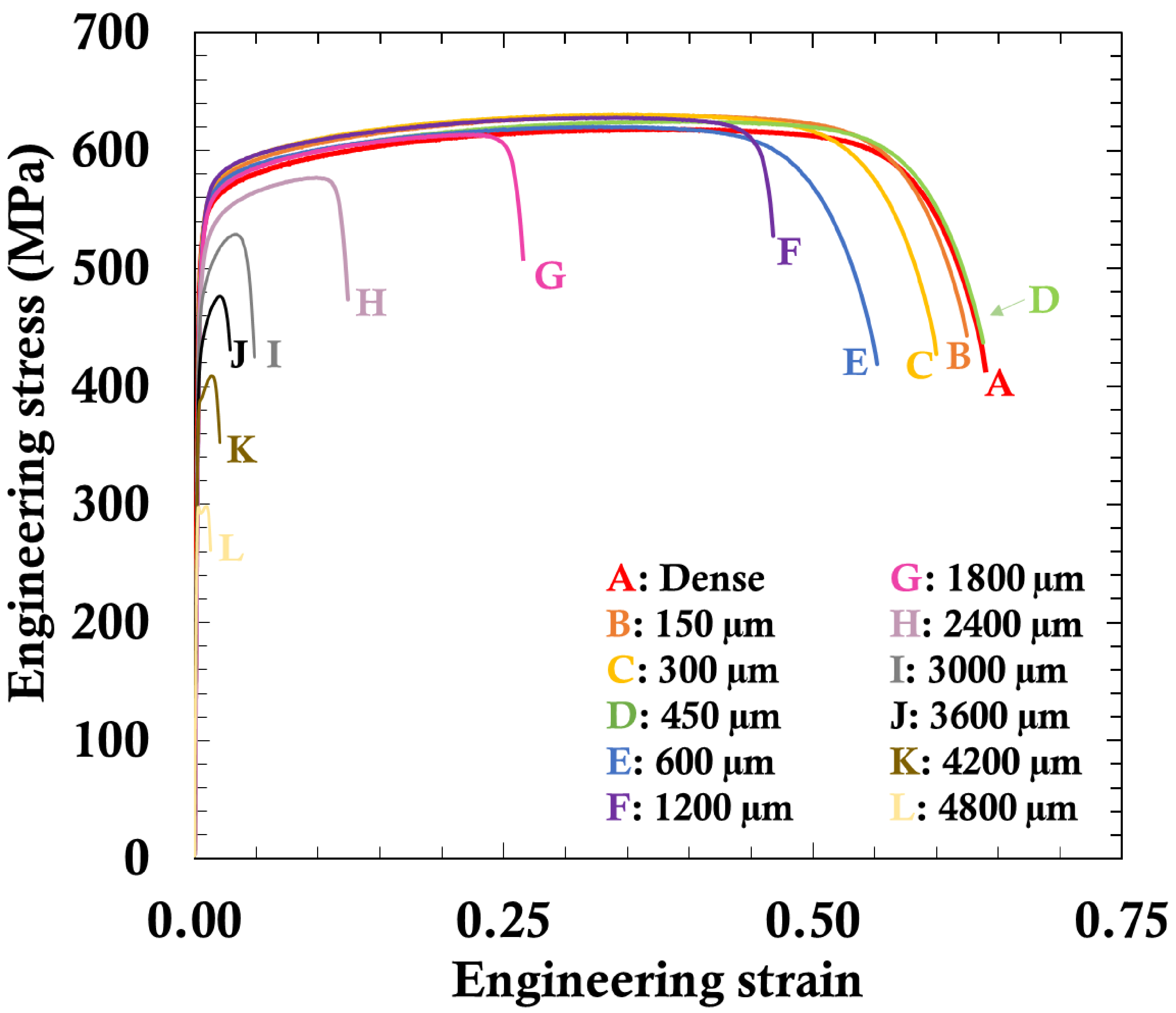

Fig. 5: Engineering stress vs. engineering strain for tensile specimens with each internal pore geometry [2]

Conclusions and Takeaways

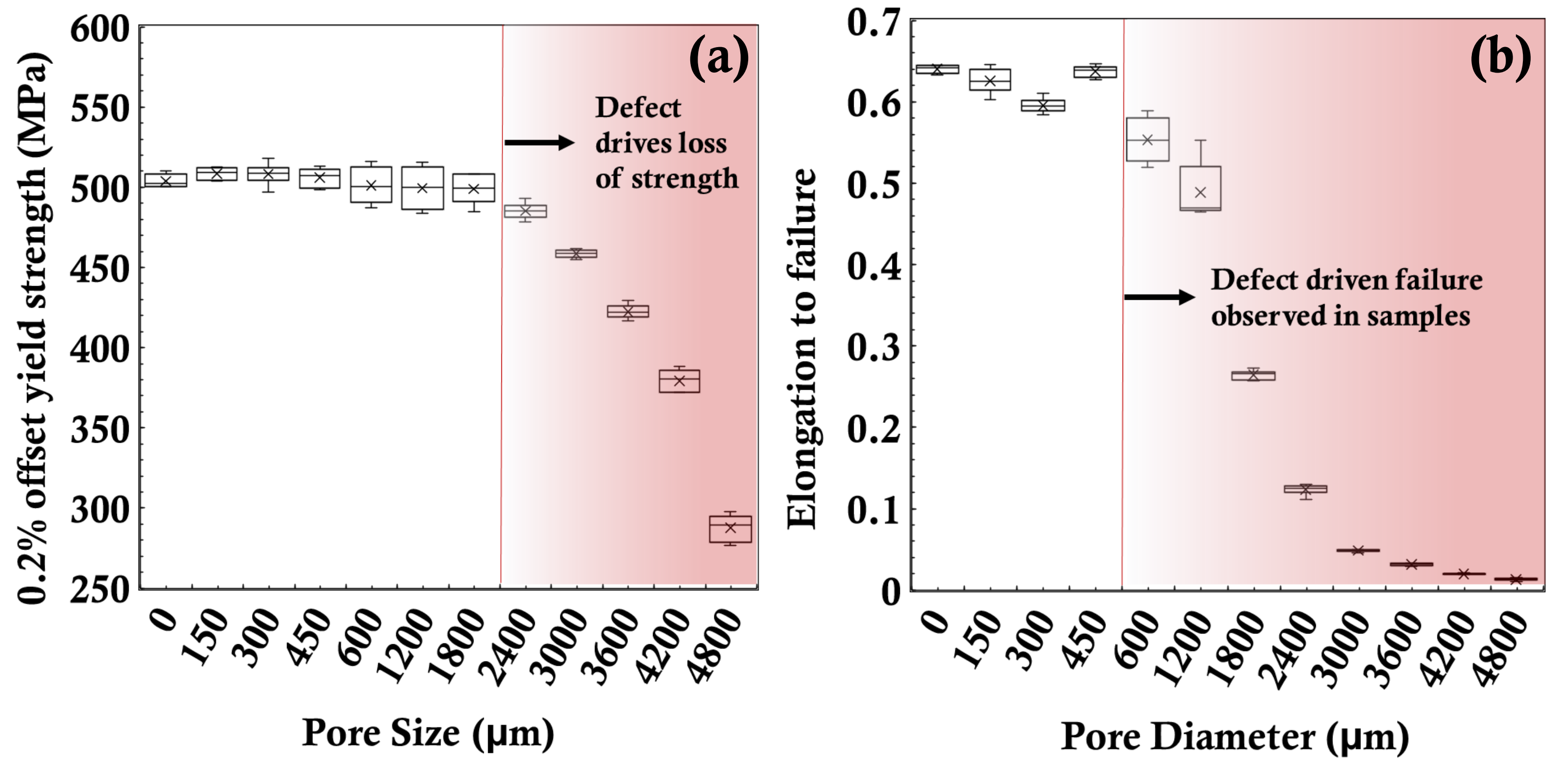

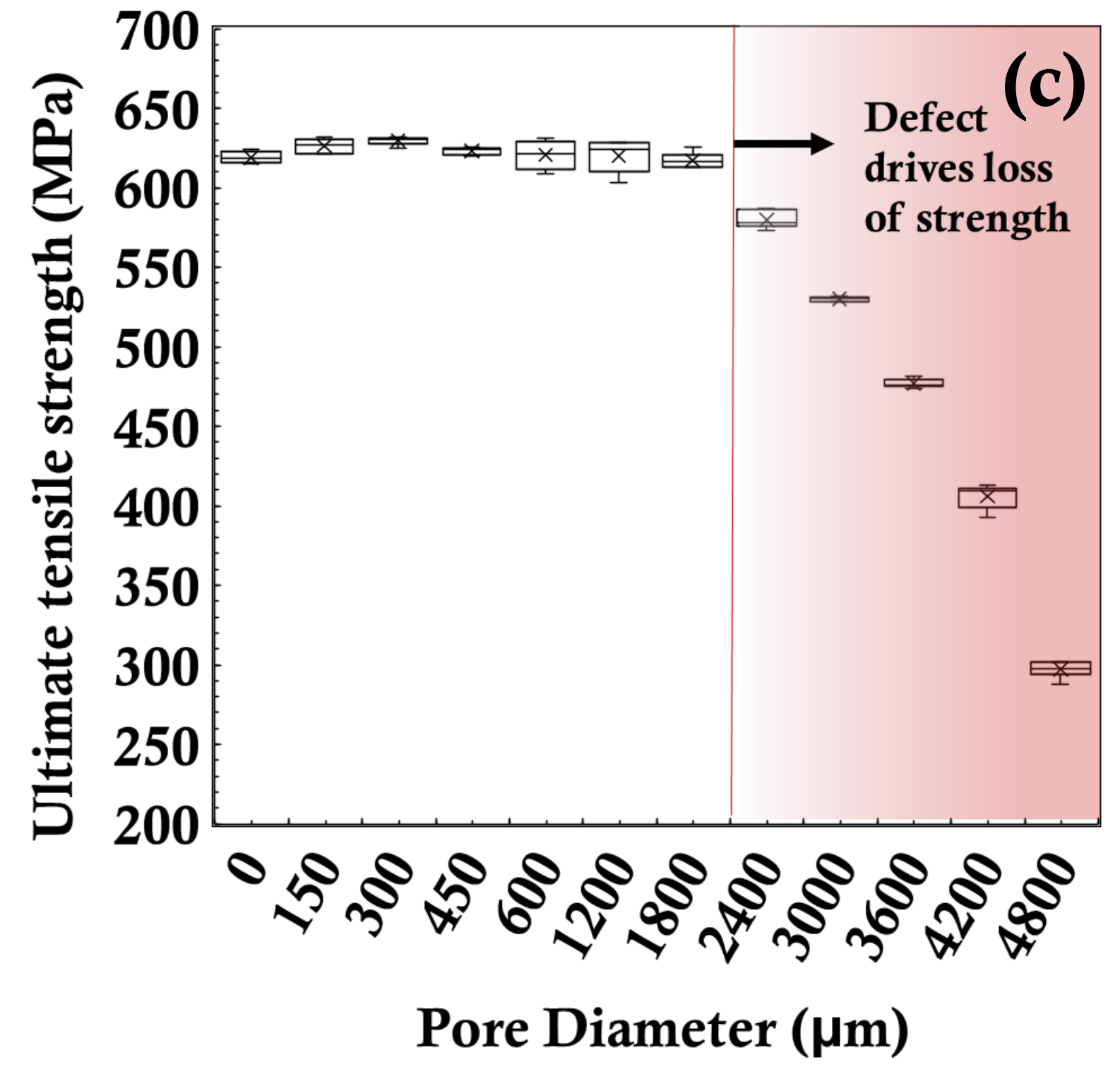

Fig. 6: Defect-driven impact of internal pore size on **(a)** Yield strength **(b)** Failure elongation **(c)** Ultimate tensile strength [2]

- X-ray CT allowed for characterization of pores based on location and morphology, proving to be the most accurate method.
- Defect-driven loss of:
  - Ultimate tensile and yield strength starting at 2400 µm pore diameter (16% of cross sectional area)
  - Elongation beginning at 1800 µm (9% of cross sectional area) pore diameter

References

[1] Frazier WE (2014) Metal Additive Manufacturing: A Review. J Mater Eng Perform 23:1917–1928. doi: 10.1007/s11665-014-0958-z

[2] A.E. Wilson-Heid, T.C. Novak, and A.M. Beese. "Characterization of the Effects of Internal Pores on Tensile Properties of Additively Manufactured Austenitic Stainless Steel 316L." *Experimental Mechanics*, vol. 59, no. 6, pp. 793–804.

Acknowledgements

This work was financially supported by the National Science Foundation under award number CMMI-1652575. The authors also gratefully acknowledge the staff of the Center for Quantitative Imagine (CQI) for their assistance with X-ray CT.